Trace Anomaly as Signature of Conformality in Neutron Stars

Yuki Fujimoto,[1,*] Kenji Fukushima,[2,†] Larry D. McLerran,[1,‡] and Michał Praszałowicz[3,1,§]
[1]Institute for Nuclear Theory, University of Washington, Box 351550, Seattle, Washington 98195, USA
[2]Department of Physics, The University of Tokyo, 7-3-1 Hongo, Bunkyo-ku, Tokyo 113-0033, Japan
[3]Institute of Theoretical Physics, Jagiellonian University, S. Łojasiewicza 11, 30-348 Kraków, Poland

(Received 2 August 2022; revised 1 November 2022; accepted 14 November 2022; published 16 December 2022)

We discuss an interpretation that a peak in the sound velocity in neutron star matter, as suggested by the observational data, signifies strongly coupled conformal matter. The normalized trace anomaly is a dimensionless measure of conformality leading to the derivative and the nonderivative contributions to the sound velocity. We find that the peak in the sound velocity is attributed to the derivative contribution from the trace anomaly that steeply approaches the conformal limit. Smooth continuity to the behavior of high-density QCD implies that the matter part of the trace anomaly may be positive definite. We discuss a possible implication of the positivity condition of the trace anomaly on the M-R relation of the neutron stars.

DOI: 10.1103/PhysRevLett.129.252702

Introduction.—Massless quantum chromodynamics (QCD) exhibits conformal symmetry, and the expectation value of the trace of the energy-momentum tensor, $\langle\Theta\rangle \equiv \langle T^{\mu}_{\mu}\rangle$, vanishes at the classical level [1]. Conformal symmetry, however, is broken at the quantum level. This violation is quantified via the trace anomaly, which has the anomalous term proportional to the gluon condensate owing to the running of the strong coupling constant α_s.

At finite temperature T and baryon chemical potential μ_B, the condensate should depend on T and μ_B and we can decompose the trace anomaly into the vacuum and the matter parts. The matter part of the trace anomaly can be expressed in terms of thermodynamic quantities, i.e., the energy density ε and the pressure P, as $\langle\Theta\rangle_{T,\mu_B} = \varepsilon - 3P$. An interesting question is how $\langle\Theta\rangle_{T,\mu_B}$ changes near the transition point. At finite T and $\mu_B/T \ll 1$ the lattice-QCD simulations provide the first-principles estimate. In Refs. [3,4] the normalized trace anomaly $(\varepsilon - 3P)/T^4$ (referred to as the interaction measure), in the pure Yang-Mills theory was found to have a sharp peak at the deconfinement temperature T_c and a tail approaching zero asymptotically at high T.

This enhancement is understood from the thermal modification of the condensate. The gluon condensate melts near the transition point leading to a peak in the thermal part of the trace anomaly. Lattice measurements of the trace anomaly have a striking impact on our understanding of deconfined matter. As pointed out in the section "Discussion of conformal symmetry" in Ref. [5] the trace anomaly behaves like $\langle\Theta\rangle_T \propto T$ even for $T \gtrsim 2T_c$ suggesting that a strongly coupled gluonic system is realized in the deconfined phase.

The trace anomaly has been also calculated in full QCD with dynamical quarks (e.g., Refs. [6–8]). The hard-thermal-loop perturbation theory (HTLpt) is successful in reproducing the trace anomaly with quarks already around $T \sim 2T_c$, while the agreement between the lattice and the HTLpt results for the pure Yang-Mills theory begins only around $T \sim 8T_c$ [9].

These high-T studies motivate us to investigate the trace anomaly at high baryon density. For baryon density $n_B > n_0$, where $n_0 \approx 0.16\ \mathrm{fm}^{-3}$ is the saturation density, QCD thermodynamics is elusive because the lattice calculations are hampered by the sign problem. The only *ab initio* methods are the chiral effective field theory (χEFT) around $n_B \sim n_0$ (see, e.g., Ref. [10] for a recent review), and the perturbative QCD (pQCD) at high density where α_s is sufficiently small [11,12] (see also Refs. [13–17] for recent developments).

To constrain thermodynamic quantities or the equation of state (EOS), we can also rely on the empirical knowledge from the neutron star (NS) observations; the sound velocity, $v_s^2 \equiv dP/d\varepsilon$, characterizes the EOS. Recently, a nonmonotonicity of v_s^2 as a function of density has been conjectured [18–20]. For instance, a quarkyonic description of dense matter [21–30] in the large-N_c limit [31,32] leads to the rapid increase, accompanied by a peak of the sound velocity (see also Refs. [33–36]).

At asymptotic densities where QCD recovers conformality, $v_s^2 \to 1/3$ is expected; this limit is commonly referred to as the conformal limit, and thus $1/3 - v_s^2$ serves a measure of conformality. There was a conjecture claiming $1/3 - v_s^2 \geq 0$ at all densities [37]; see also Ref. [38]. However, the recent analyses of NS data including the two-solar-mass pulsars [39–42] are in strong tension with $1/3 - v_s^2 \geq 0$ at sufficiently high n_B [43–47], which seems to challenge the conformality in dense NS matter in deep cores.

Here, we propose the trace anomaly scaled by the energy density as a new measure of conformality. The sound velocity is expressed solely in terms of the normalized trace anomaly, and the latter is a more comprehensive quantity than v_s^2. Here, we extract the trace anomaly from the EOSs inferred from the NS data [45,48–50]. We discuss the conformal limits $\langle\Theta\rangle_{T,\mu_B} \to 0$ and $v_s^2 \to 1/3$, and clarify the difference. We show that the enhancement in the sound velocity is not in contradiction with conformality. We then discuss the possibility that the trace anomaly is positive definite at all densities. We give a number of arguments for the positivity of the trace anomaly and discuss implications for NS physics.

Trace anomaly at finite baryon density.—Scale transformations lead to the dilatation current $j_D^\nu = x_\mu T^{\mu\nu}$ for which $\partial_\nu j_D^\nu = T_\mu^\mu = \Theta$ [51]. For conformal theories $\Theta = 0$ but in QCD both quark masses and the trace anomaly explicitly break the scale invariance as [52,53]

$$\Theta = \frac{\beta}{2g} F_{\mu\nu}^a F_a^{\mu\nu} + (1+\gamma_m)\sum_f m_f \bar{q}_f q_f, \tag{1}$$

where $\beta/2g = -(11 - 2N_f/3)\alpha_s/8\pi + \mathcal{O}(\alpha_s^2)$ is the QCD beta function and $\gamma_m = 2\alpha_s/\pi + \mathcal{O}(\alpha_s^2)$ is the anomalous dimension of the quark mass.

At finite T and/or μ_B, the expectation value involves a matter contribution as $\langle\Theta\rangle = \langle\Theta\rangle_{T,\mu_B} + \langle\Theta\rangle_0$ where $\langle\Theta\rangle_0$ represents the vacuum expectation value at $T = \mu_B = 0$. In this Letter, we will focus on the matter contribution only given by

$$\langle\Theta\rangle_{T,\mu_B} = \varepsilon - 3P. \tag{2}$$

It is customary to call $\langle\Theta\rangle_{T,\mu_B}$ the trace anomaly too. If thermal degrees of freedom are dominated by massless particles as is the case in the high-T limit, the Stefan-Boltzmann law is saturated and $P \sim T^4$ at high temperature or $P \sim \mu_B^4$ at high density, so that $\varepsilon = 3P$. Conversely, using thermodynamic relations, one can show that $\langle\Theta\rangle_{T,\mu_B} = 0$ implies $P \propto T^4$ or $P \propto \mu_B^4$, respectively. Thus, $\langle\Theta\rangle_{T,\mu_B}$ is a probe for the thermodynamic content of matter.

The physical meaning of the trace anomaly is transparent from the following relations:

$$\frac{\langle\Theta\rangle_{T,\mu_B=0}}{T^4} = T\frac{d\nu_T}{dT}, \qquad \frac{\langle\Theta\rangle_{T=0,\mu_B}}{\mu_B^4} = \mu_B\frac{d\nu_\mu}{d\mu_B}, \tag{3}$$

where we quantify the effective degrees freedom by $\nu_T \equiv P/T^4$ and $\nu_\mu \equiv P/\mu_B^4$ for hot matter at $\mu_B = 0$ and dense matter at $T = 0$, respectively. These imply that the trace anomaly is proportional to the increasing rate of the thermal degrees of freedom as the temperature or density grows up.

Here, we propose to use

$$\Delta \equiv \frac{\langle\Theta\rangle_{T,\mu_B}}{3\varepsilon} = \frac{1}{3} - \frac{P}{\varepsilon} \tag{4}$$

as a measure of the trace anomaly [54]. The thermodynamic stability and the causality require $P > 0$ and $P \le \varepsilon$, respectively. Therefore, $-2/3 \le \Delta < 1/3$, and $\Delta \to 0$ in the scale-invariant limit.

We decompose the sound velocity as

$$v_s^2 = \frac{dP}{d\varepsilon} = v_{s,\mathrm{deriv}}^2 + v_{s,\mathrm{nonderiv}}^2, \tag{5}$$

where the derivative and the nonderivative terms are

$$v_{s,\mathrm{deriv}}^2 \equiv -\frac{d\Delta}{d\eta}, \qquad v_{s,\mathrm{nonderiv}}^2 \equiv \frac{1}{3} - \Delta. \tag{6}$$

Here, $\eta \equiv \ln(\varepsilon/\varepsilon_0)$ and ε_0 is the energy density at nuclear saturation density, i.e., $\varepsilon_0 = 150\ \mathrm{MeV/fm^3}$. From these expressions it is evident that the restoration of conformality renders $\Delta \to 0$ and $d\Delta/d\eta \to 0$, so that $v_s^2 \simeq v_{s,\mathrm{nonderiv}}^2 \to 1/3$ in the conformal limit at asymptotically high density.

Trace anomaly from the NS observations.—In Fig. 1, we show Δ extracted from various $P(\varepsilon)$ constrained by NS observables [45,48–50]. The error band represents the 1σ credible interval corresponding to the error in $P(\varepsilon)$. Since ε is treated as an explanatory variable, the relative error in $\Delta(\varepsilon)$ is assumed to be the same as that in $P(\varepsilon)$.

For all these data $\Delta \sim 0$ within the error at relatively low energy density. Note that the red dash-dotted curve in Fig. 1

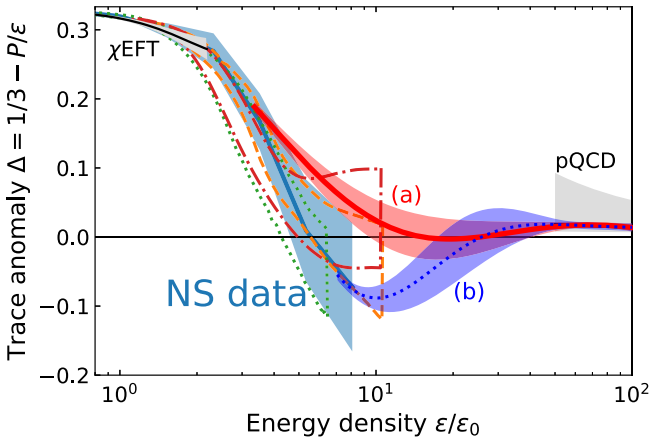

FIG. 1. Normalized trace anomaly readout from four independent EOSs inferred from NS data; the light blue solid line and error band from Ref. [45], the orange dashed lines from Ref. [48], the green dotted lines from Ref. [49], and the red dot-dashed lines from Ref. [50]. We show two *ab initio* calculations (χEFT [46] and pQCD [12]) and the red line marked as (a) and the blue dotted line marked as (b) are interpolations with 1σ band by the Gaussian process applied to different regions of NS data.

follows from the analysis including pQCD as an input [50], which makes the tendency $\Delta \sim 0$ more apparent.

Figure 1 shows that the (normalized) trace anomaly in the present experimental range monotonically decreases with increasing ε. At asymptotically high density $\Delta \to 0$ should be eventually reached. It is nontrivial that the NS observations favor $\Delta \sim 0$ at intermediate ε, well below the asymptotic density. Here, we elucidate that this quick approach to conformality causes a prominent peak in v_s^2. We emphasize that, even if the behavior toward $\Delta \to 0$ is monotonic in ε, $v_s^2 > 1/3$ can be induced.

The minimal parametrization of monotonically decreasing Δ is

$$\Delta = \frac{1}{3} - \frac{1}{3}\frac{1}{e^{-\kappa(\eta-\eta_c)}+1}\left(1 - \frac{A}{B+\eta^2}\right). \tag{7}$$

The crossover density to conformal matter is characterized by η_c and the width of the crossover region is $1/\kappa$. Equation (7) has the correct limit $\Delta \to 1/3$ for $\eta \ll \eta_c$ and $\Delta \sim (A/3)/(B+\eta^2) \to 0$ for $\eta \gg \eta_c$. Nonzero A and B represent the pQCD logarithmic tails that are not well constrained from the NS data. One parameter set that fits the observational data reads

$$\kappa = 3.45, \qquad \eta_c = 1.2 \qquad A = 2, \qquad B = 20. \tag{8}$$

The fit together with data is shown in the inset plot in Fig. 2. We show v_s^2 computed from Eq. (5) with the help of Eq. (7) in Fig. 2. In the high density region for $\eta \gtrsim 2$, v_s^2 is dominated by $v_{s,\mathrm{nonderiv}}^2$ approaching the conformal value, $1/3$. At low density for $\eta \lesssim 1$, v_s^2 goes to zero.

The most interesting is the behavior of v_s^2 around $1 \lesssim \eta \lesssim 2$. This density region corresponds to the energy scale of the transitional change from nonrelativistic to relativistic degrees of freedom. There, v_s^2 develops a peak whose height can become larger than the conformal value.

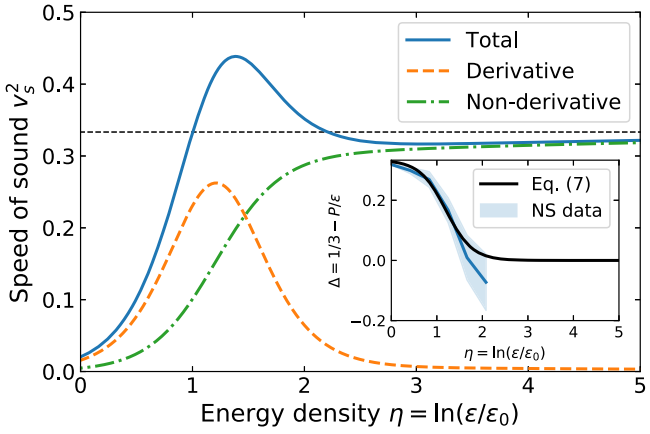

FIG. 2. The speed of sound and its decomposition (6) calculated from (7) as shown in the inset plot. The horizontal axis is the logarithmic energy η normalized to the value at the saturation point $\varepsilon_0 = 150\ \mathrm{MeV/fm^3}$.

The dashed and the dash-dotted lines in Fig. 2 show $v_{s,\mathrm{deriv}}^2$ and $v_{s,\mathrm{nonderiv}}^2$, respectively. Because Δ of Eq. (7) is a monotonic function, $v_{s,\mathrm{nonderiv}}^2$ smoothly increases with increasing η. Thus, $v_{s,\mathrm{deriv}}^2$ exhibits the peak structure. From this decomposition we clearly recognize that the peak in v_s^2 is not caused by the violation of the conformal bound, but it is a signature of the steep approach to the conformal limit.

We stress that this is quite different from high-T QCD where the normalized trace anomaly itself has a peak around T_c, which causes a *minimum* in the sound velocity. Along the T axis conformality is restored only at temperatures *far above* T_c. One might have an impression that conformality in QCD should be associated with the weak coupling, but it is not necessarily the case. What we find from Fig. 1 is that conformality quantified by Δ is quickly restored around $1 \lesssim \eta \lesssim 2$ and the peak in v_s^2 should be interpreted as a signature of conformality. The peak position may well be identified as the point of the slope change as observed in Ref. [56]. Around this peak α_s is not yet small and the state of matter for $\eta \gtrsim 2$ should be regarded as "strongly coupled conformal matter."

We note that $v_s^2 \to 1/3$ generally occurs at lower density than $\Delta \to 0$. We can illustrate this in a simple model with the vector interaction between the currents whose energy density is given by

$$\varepsilon(n) = m_N n_B + \frac{C}{\Lambda^2} n_B^2, \tag{9}$$

where $m_N = N_c \Lambda_{\mathrm{QCD}}$ is the baryon mass, and C and Λ are the typical interaction strength and the scale of the system, respectively. This can be thought of as the generalization of the mean-field quantum hadrodynamics [57]. Note that $\mu_B = m_N + 2(C/\Lambda^2)n_B$, and $P = (C/\Lambda^2)n_B^2$. This means that $\Theta = m_N n_B - 2(C/\Lambda^2)n_B^2$ and $v_s^2 = 2(C/\Lambda^2)n_B/[m_N + 2(C/\Lambda^2)n_B]$. The conformal point $\Delta \to 0$ is reached when $n_B \sim N_c \Lambda_{\mathrm{QCD}}^3/(2C)$. The condition of $v_s^2 \to 1/3$ is reached earlier at $n_B \sim N_c \Lambda_{\mathrm{QCD}}^3/(4C)$. So in this model the density at which v_s^2 surpasses the conformal limit is always lower than that for the trace anomaly.

Strongly coupled conformal matter.—In Fig. 1 we overlay the currently available *ab initio* calculations of χEFT [46] and pQCD [12] on the observational data that, however, do not constrain Δ beyond $\varepsilon/\varepsilon_0 \sim 10^1$. We utilized the Gaussian process for the interpolation using NS data from the machine learning [45] up to the density $\varepsilon/\varepsilon_0 \lesssim 4$ (a) and using all data up to $\varepsilon/\varepsilon_0 \sim 8$ (b). Details about the choice of the kernel and the noise will be reported elsewhere.

In the conservative inference in (a) Δ stays positive or slightly negative after quickly approaching zero, which implies a possible bound, $\Delta \geq 0$. Once the conformal limit

of the trace anomaly is saturated, the underlying theory becomes approximately scale invariant and the EOS drastically simplifies. Baryons are strongly interacting, and yet the resultant EOS of strongly coupled conformal matter is $P \approx \varepsilon/3$.

If the mean value from the machine learning inference is extrapolated, the Gaussian process prefers (b). In this case Δ has a nonmonotonic structure with two nodes. Accordingly, there should be a density window with $d\Delta/d\varepsilon > 0$ (i.e., $v^2_{s,(\mathrm{deriv})} < 0$) between the two zeros. The peak in v_s^2 is hardly affected, however, the maximum of v_s^2 is pulled up as compared to (a). If $v^2_{s,(\mathrm{deriv})}$ happens to be negative large, v_s^2 approaches zero after the peak, which causes softening of the EOS similarly to the first-order phase transition. Intuitively, the peak in v_s^2 is generated by EOS stiffening, but the soft pQCD EOS at high density requires EOS softening at intermediate density.

Is the trace anomaly positive in finite-density QCD?.— Let us focus on the scenario (a) and consider its implications. The smooth curve of (a) in Fig. 1 supports a hypothetical relation, $\langle\Theta\rangle_{\mu_B} \geq 0$ (equivalently, $P \leq \varepsilon/3$). The positivity condition of the QCD trace anomaly has been often assumed in the literature of finite-T QCD; see, e.g., Ref. [58]. The lattice-QCD calculations at finite T give thermodynamic quantities satisfying $\langle\Theta\rangle_T \geq 0$ [6–8].

In general, however, the trace anomaly may not be positive definite. For example, if the low-energy theory is a gauge theory governed by a free infrared (IR) fixed point such as an Abelian gauge theory with massless fermions or a non-Abelian gauge theory with many massless flavors [59], where the β function is positive at weak coupling and $\langle F^2\rangle$ is known to be negative, then the trace anomaly (1) becomes negative. We also point out that some phenomenological nuclear EOSs bear a negative trace anomaly due to sudden stiffening of the EOS with $P > \varepsilon/3$ [57,60,61]. Moreover, QCD at finite isospin chemical potential [62] and two-color QCD at finite μ_B [63,64] produce a negative trace anomaly.

Nevertheless, in view of the observational data in Fig. 1, QCD may well enjoy a special property that the matter part of the trace anomaly is positive definite. One supportive argument is based on the behavior of the chromoelectric field $\boldsymbol{E}$ and the chromomagnetic field $\boldsymbol{B}$. In the chiral limit only the gluon condensate, $\langle F^2\rangle_{\mu_B} = \langle \boldsymbol{B}^2 - \boldsymbol{E}^2\rangle_{\mu_B}$, contributes to the trace anomaly. Nuclear matter at low density is approximated as a gas of nucleons, and the trace anomaly is positive for each nucleon (that is the nucleon mass squared), and so the trace anomaly in dilute nuclear matter should be positive. In the nonrelativistic quark model at higher density, the interquark interaction is dominantly mediated by the chromoelectric field, and so the trace anomaly is positive. Besides, we know for sure that the direct pQCD computation at asymptotic high density gives a positive trace anomaly.

From another perspective the positivity of the trace anomaly can be motivated as follows. Equation (3) relates the matter part of the trace anomaly to the density derivative of effective degrees of freedom ν_μ. As long as more effective degrees of freedom are liberated at higher μ_B, we can conclude $\langle\Theta\rangle_{\mu_B} \geq 0$ because of $d\nu_\mu/d\mu_B \geq 0$. It is an intriguing question how the above argument could be modified if color superconductivity is activated with a finite condensation of quark Cooper pairs.

To prove $\langle\Theta\rangle_{\mu_B} \geq 0$ directly from QCD is an intriguing challenge. It is a nontrivial and profound question due to the composite operator renormalization. Here, we propose a complementary strategy to test this conjectured inequality using astronomical observations of NSs, namely, the maximum mass bound.

One-to-one correspondence is established between the EOS and $M(R)$ (where M is the NS mass as a function of the NS radius R). In order to find the maximum mass, $M_{\mathrm{max}}(R)$, for a given radius R. we assume a standard crust EOS up to $n_B \leq 0.5 n_0$ [65,66]. Then, for $n_B > 0.5 n_0$ we identify $M_{\mathrm{max}}(R)$ by taking the maximally stiff or soft EOS parametrizations. Technical details are outlined in Refs. [67,68] (see also Ref. [46]).

Some maximally stiff EOS may render negative Δ. In Fig. 3 the dotted line represents the original $M_{\mathrm{max}}(R)$, while the black solid line shows $M_{\mathrm{max}}(R)$ for the EOS with the $\Delta \geq 0$ condition taken into account. Performing the EOS scan we find the gray shaded region that is incompatible with the $\Delta \geq 0$ condition. For completeness we overlay three current radius measurements obtained with two different methods; namely, spectral measurement of 4U 1820-30 and SAX J1748.9-2021 [69], as well as the timing measurement of J0740 + 6620 from NICER [70,71]. We also plot the M-R relations from empirical nuclear EOSs [61,72–75]. From Fig. 3 we can say that the $\Delta \geq 0$ condition has a phenomenological impact to tighten

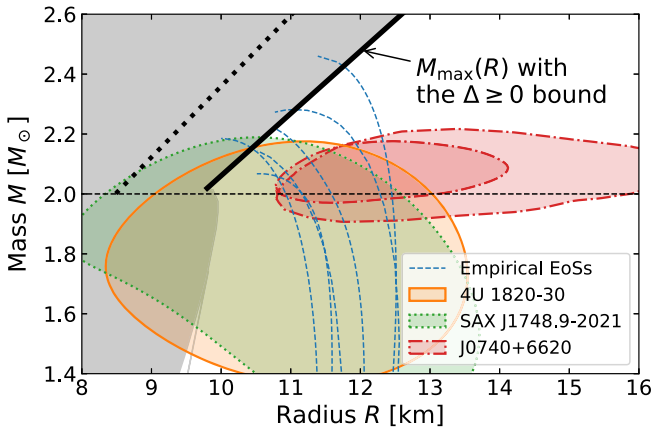

FIG. 3. The effect of the $\Delta \geq 0$ bound on the NS M-R relation. The black solid (dotted) line shows the maximum mass configuration for the EOS with (without) the $\Delta \geq 0$ bound. We also overlay the measurement of NSs and the M-R relations (thin dashed curves) corresponding to empirical nuclear EOSs from Refs. [61,72–74] and two variants from Refs. [75,83].

the allowed M-R region. In Fig. 3 we put a thin line at $M/M_\odot = 2$ as a guide for the eye. If the maximum mass is larger as reported in Refs. [42,76], our proposed bound would exclude EOSs that lead to sufficiently heavy mass but small R inside the gray shaded region. We propose further systematic comparisons of results with and without our positivity condition as well as the hypothesised conformality bound on the sound velocity for other observables such as the tidal deformability along the lines of, e.g., Refs. [77,78]. Future multimessenger observations, which are expected to pin down the maximum mass of NSs [79–82], and radius measurements together with the tidal deformability inferred from the merger will help to test our conjecture of the positive trace anomaly.

We thank Neill Warrington for discussions. Y. F. would like to acknowledge useful conversations with Greg Jackson and Sanjay Reddy. K. F. thanks Shi Chen for illuminating discussions. The work of Y. F., L. M., and M. P. was supported by the U.S. DOE under Grant No. DE-FG02-00ER41132. K. F. was supported by JSPS KAKENHI Grants No. 22H01216 and No. 22H05118.

*yfuji@uw.edu
†fuku@nt.phys.s.u-tokyo.ac.jp
‡mclerran@me.com
§michal.praszalowicz@uj.edu.pl

[1] For the non-Abelian gauge theories coupled to fermions scale invariance implies conformality; see Ref. [2]. Throughout this paper *conformality* means $\langle\Theta\rangle = 0$. Conversely, we dub $\langle\Theta\rangle \neq 0$ as a *trace anomaly*.
[2] J. Polchinski, Phys. Rev. D **27**, 1320 (1983).
[3] G. Boyd, J. Engels, F. Karsch, E. Laermann, C. Legeland, M. Lutgemeier, and B. Petersson, Phys. Rev. Lett. **75**, 4169 (1995).
[4] G. Boyd, J. Engels, F. Karsch, E. Laermann, C. Legeland, M. Lutgemeier, and B. Petersson, Nucl. Phys. **B469**, 419 (1996).
[5] D. E. Miller, Phys. Rep. **443**, 55 (2007).
[6] M. Cheng *et al.*, Phys. Rev. D **77**, 014511 (2008).
[7] S. Borsanyi, Z. Fodor, C. Hoelbling, S. D. Katz, S. Krieg, and K. K. Szabo, Phys. Lett. B **730**, 99 (2014).
[8] A. Bazavov, T. Bhattacharya, C. DeTar, H. T. Ding, S. Gottlieb *et al.* (HotQCD Collaboration), Phys. Rev. D **90**, 094503 (2014).
[9] J. O. Andersen, L. E. Leganger, M. Strickland, and N. Su, Phys. Rev. D **84**, 087703 (2011).
[10] C. Drischler, J. W. Holt, and C. Wellenhofer, Annu. Rev. Nucl. Part. Sci. **71**, 403 (2021).
[11] B. A. Freedman and L. D. McLerran, Phys. Rev. D **16**, 1130 (1977); **16**, 1147 (1977); **16**, 1169 (1977).
[12] A. Kurkela, P. Romatschke, and A. Vuorinen, Phys. Rev. D **81**, 105021 (2010).
[13] T. Gorda, A. Kurkela, P. Romatschke, S. Säppi, and A. Vuorinen, Phys. Rev. Lett. **121**, 202701 (2018).
[14] T. Gorda, A. Kurkela, R. Paatelainen, S. Säppi, and A. Vuorinen, Phys. Rev. Lett. **127**, 162003 (2021); Phys. Rev. D **104**, 074015 (2021).
[15] T. Gorda, A. Kurkela, J. Österman, R. Paatelainen, S. Säppi, P. Schicho, K. Seppänen, and A. Vuorinen, arXiv:2204.11279. (2022).
[16] Y. Fujimoto and K. Fukushima, Phys. Rev. D **105**, 014025 (2022).
[17] L. Fernandez and J.-L. Kneur, arXiv:2109.02410 [Phys. Rev. Lett. (to be published)].
[18] T. Kojo, AAPPS Bull. **31**, 11 (2021).
[19] S. Altiparmak, C. Ecker, and L. Rezzolla, arXiv:2203.14974.
[20] C. Ecker and L. Rezzolla, arXiv:2207.04417.
[21] L. McLerran and R. D. Pisarski, Nucl. Phys. **A796**, 83 (2007).
[22] D. C. Duarte, S. Hernandez-Ortiz, K. S. Jeong, and L. D. McLerran, Phys. Rev. D **104**, L091901 (2021).
[23] T. Kojo, Phys. Rev. D **104**, 074005 (2021).
[24] T. Kojo and D. Suenaga, Phys. Rev. D **105**, 076001 (2022).
[25] K. Fukushima and T. Kojo, Astrophys. J. **817**, 180 (2016).
[26] L. McLerran and S. Reddy, Phys. Rev. Lett. **122**, 122701 (2019).
[27] K. S. Jeong, L. McLerran, and S. Sen, Phys. Rev. C **101**, 035201 (2020).
[28] S. Sen and N. C. Warrington, Nucl. Phys. **A1006**, 122059 (2021).
[29] G. Cao and J. Liao, J. High Energy Phys. 10 (2020) 168.
[30] N. Kovensky and A. Schmitt, J. High Energy Phys. 09 (2020) 112.
[31] G. 't Hooft, Nucl. Phys. **B72**, 461 (1974).
[32] E. Witten, Nucl. Phys. **B160**, 57 (1979).
[33] R. D. Pisarski, Phys. Rev. D **103**, L071504 (2021).
[34] M. Hippert, E. S. Fraga, and J. Noronha, Phys. Rev. D **104**, 034011 (2021).
[35] H. K. Lee, Y.-L. Ma, W.-G. Paeng, and M. Rho, Mod. Phys. Lett. A **37**, 2230003 (2022).
[36] M. Marczenko, L. McLerran, K. Redlich, and C. Sasaki, arXiv:2207.13059.
[37] A. Cherman, T. D. Cohen, and A. Nellore, Phys. Rev. D **80**, 066003 (2009).
[38] P. M. Hohler and M. A. Stephanov, Phys. Rev. D **80**, 066002 (2009).
[39] P. Demorest, T. Pennucci, S. Ransom, M. Roberts, and J. Hessels, Nature (London) **467**, 1081 (2010); E. Fonseca *et al.*, Astrophys. J. **832**, 167 (2016).
[40] J. Antoniadis *et al.*, Science **340**, 6131 (2013).
[41] H. T. Cromartie *et al.* (NANOGrav Collaboration), Nat. Astron. **4**, 72 (2020); E. Fonseca *et al.*, Astrophys. J. Lett. **915**, L12 (2021).
[42] R. W. Romani, D. Kandel, A. V. Filippenko, T. G. Brink, and W. Zheng, Astrophys. J. Lett. **934**, L18 (2022).
[43] P. Bedaque and A. W. Steiner, Phys. Rev. Lett. **114**, 031103 (2015).
[44] I. Tews, J. Carlson, S. Gandolfi, and S. Reddy, Astrophys. J. **860**, 149 (2018).
[45] Y. Fujimoto, K. Fukushima, and K. Murase, Phys. Rev. D **98**, 023019 (2018); **101**, 054016 (2020); J. High Energy Phys. 03 (2021) 273.

[46] C. Drischler, S. Han, J. M. Lattimer, M. Prakash, S. Reddy, and T. Zhao, Phys. Rev. C **103**, 045808 (2021).
[47] C. Drischler, S. Han, and S. Reddy, Phys. Rev. C **105**, 035808 (2022).
[48] M. Al-Mamun, A. W. Steiner, J. Nättilä, J. Lange, R. O'Shaughnessy, I. Tews, S. Gandolfi, C. Heinke, and S. Han, Phys. Rev. Lett. **126**, 061101 (2021).
[49] G. Raaijmakers, S. K. Greif, K. Hebeler, T. Hinderer, S. Nissanke, A. Schwenk, T. E. Riley, A. L. Watts, J. M. Lattimer, and W. C. G. Ho, Astrophys. J. Lett. **918**, L29 (2021).
[50] T. Gorda, O. Komoltsev, and A. Kurkela, arXiv:2204.11877.
[51] S. Coleman, *Aspects of Symmetry: Selected Erice Lectures* (Cambridge University Press, Cambridge, U.K., 1985).
[52] J. C. Collins, A. Duncan, and S. D. Joglekar, Phys. Rev. D **16**, 438 (1977).
[53] N. K. Nielsen, Nucl. Phys. **B120**, 212 (1977).
[54] Our Δ is equivalent to $\mathcal{C}$ defined in Ref. [55] apart from an overall constant, $1/3$.
[55] R. V. Gavai, S. Gupta, and S. Mukherjee, Phys. Rev. D **71**, 074013 (2005).
[56] E. Annala, T. Gorda, A. Kurkela, J. Nättilä, and A. Vuorinen, Nat. Phys. **16**, 907 (2020).
[57] B. D. Serot and J. D. Walecka, Int. J. Mod. Phys. E **06**, 515 (1997).
[58] J. D. Bjorken, Phys. Rev. D **27**, 140 (1983).
[59] T. Appelquist, A. G. Cohen, and M. Schmaltz, Phys. Rev. D **60**, 045003 (1999).
[60] Y. B. Zel'dovich, Zh. Eksp. Teor. Fiz. **41**, 1609 (1961).
[61] A. Akmal, V. R. Pandharipande, and D. G. Ravenhall, Phys. Rev. C **58**, 1804 (1998).
[62] D. T. Son and M. A. Stephanov, Phys. Rev. Lett. **86**, 592 (2001); Phys. At. Nucl. **64**, 834 (2001).
[63] S. Cotter, P. Giudice, S. Hands, and J.-I. Skullerud, Phys. Rev. D **87**, 034507 (2013).
[64] K. Iida and E. Itou, arXiv:2207.01253.
[65] G. Baym, C. Pethick, and P. Sutherland, Astrophys. J. **170**, 299 (1971).
[66] J. W. Negele and D. Vautherin, Nucl. Phys. **A207**, 298 (1973).
[67] C. E. Rhoades, Jr. and R. Ruffini, Phys. Rev. Lett. **32**, 324 (1974).
[68] S. Koranda, N. Stergioulas, and J. L. Friedman, Astrophys. J. **488**, 799 (1997).
[69] F. Özel, D. Psaltis, T. Güver, G. Baym, C. Heinke, and S. Guillot, Astrophys. J. **820**, 28 (2016).
[70] T. E. Riley *et al.*, Astrophys. J. Lett. **918**, L27 (2021).
[71] M. C. Miller *et al.*, Astrophys. J. Lett. **918**, L28 (2021).
[72] S. Goriely, N. Chamel, and J. M. Pearson, Phys. Rev. C **82**, 035804 (2010).
[73] L. Engvik, G. Bao, M. Hjorth-Jensen, E. Osnes, and E. Ostgaard, Astrophys. J. **469**, 794 (1996).
[74] G. Baym, S. Furusawa, T. Hatsuda, T. Kojo, and H. Togashi, Astrophys. J. **885**, 42 (2019).
[75] H. Müther, M. Prakash, and T. L. Ainsworth, Phys. Lett. B **199**, 469 (1987).
[76] M. Linares, T. Shahbaz, and J. Casares, Astrophys. J. **859**, 54 (2018).
[77] E. Annala, T. Gorda, A. Kurkela, and A. Vuorinen, Phys. Rev. Lett. **120**, 172703 (2018).
[78] E. Annala, T. Gorda, E. Katerini, A. Kurkela, J. Nättilä, V. Paschalidis, and A. Vuorinen, Phys. Rev. X **12**, 011058 (2022).
[79] B. Margalit and B. D. Metzger, Astrophys. J. Lett. **850**, L19 (2017).
[80] M. Shibata, S. Fujibayashi, K. Hotokezaka, K. Kiuchi, K. Kyutoku, Y. Sekiguchi, and M. Tanaka, Phys. Rev. D **96**, 123012 (2017).
[81] L. Rezzolla, E. R. Most, and L. R. Weih, Astrophys. J. Lett. **852**, L25 (2018).
[82] M. Ruiz, S. L. Shapiro, and A. Tsokaros, Phys. Rev. D **97**, 021501(R) (2018).
[83] The data are adopted from http://xtreme.as.arizona.edu/NeutronStars/.